



## Drying kinetics and technological properties of corn starch extracted by ultrasonic energy<sup>1</sup>

### Cinética da secagem e caracterização tecnológica do amido de milho extraído por energia ultrassônica

Aparecida S. Taques<sup>2</sup>, Juliana A. Célia<sup>2</sup>, Daniel E. Cabral de Oliveira<sup>2</sup>, Geraldo A. Mabasso<sup>2</sup>,  
Raquel A. Loss<sup>3</sup>, Osvaldo Resende<sup>2</sup>

<sup>1</sup> Research developed at Instituto Federal de Educação, Ciência e Tecnologia Goiano. Rio Verde, GO, Brazil

<sup>2</sup> Instituto Federal de Educação, Ciência e Tecnologia Goiano. Rio Verde, GO, Brazil

<sup>3</sup> Universidade do Estado de Mato Grosso. Barra do Bugres, MT, Brazil

#### HIGHLIGHTS:

*Drying temperature affected the size of the starch granules.*

*Ultrasonic technology promoted changes in the gelatinization peaks.*

*Ultrasound treatment alters the physicochemical properties of corn starch compared to conventional extraction.*

**ABSTRACT:** Corn starch is widely used in the food industry but presents limitations in its native form, such as low thermal stability and retrogradation tendency. This study aimed to describe the drying behavior of corn starch extracted by ultrasound and evaluate its structural and technological properties after drying. Drying was carried out in a forced-air oven at 40, 50, 60, and 70 °C, and eleven mathematical models were fitted to the data. Starch was obtained by ultrasound-assisted extraction using 40 kHz, 60% amplitude for 60 min at 25 °C, followed by successive washings with distilled water. The Wang & Singh model best described drying at 40 °C, while the Midilli model was most adequate at higher temperatures. The effective diffusion coefficient ( $2.41 \times 10^{-9}$  to  $7.11 \times 10^{-9} \text{ m}^2 \text{ s}^{-1}$ ) increased linearly with temperature. The calculated activation energy was 32.25 kJ mol<sup>-1</sup>. It is concluded that drying above 50 °C is not recommended when the goal is to preserve starch quality.

**Key words:** *Zea mays*, sonication, effective diffusivity, activation energy

**RESUMO:** O amido de milho é amplamente utilizado na indústria de alimentos, mas apresenta limitações em sua forma nativa, como baixa estabilidade térmica e tendência à retrogradação. Este estudo teve como objetivo descrever a secagem do amido de milho extraído por ultrassom e avaliar suas propriedades estruturais e tecnológicas após o processo. A secagem foi realizada em estufa de circulação forçada a 40, 50, 60 e 70 °C, e onze modelos matemáticos foram ajustados aos dados. O amido foi obtido por extração assistida por ultrassom, empregando frequência de 40 kHz, 60% amplitude por 60 min a 25 °C seguida de lavagens sucessivas com água destilada. O modelo de Wang & Singh apresentou melhor ajuste a 40 °C, enquanto o de Midilli foi mais adequado nas demais temperaturas. O coeficiente de difusão efetivo ( $2,41 \times 10^{-9}$  a  $7,11 \times 10^{-9} \text{ m}^2 \text{ s}^{-1}$ ) aumentou linearmente com a temperatura, com energia de ativação de 32,25 kJ mol<sup>-1</sup>. O tamanho dos grânulos diminuiu com o aumento da temperatura, enquanto as propriedades de gelatinização foram preservadas a 40 e 50 °C. Conclui-se que a secagem acima de 50 °C não é recomendada para preservar a qualidade do amido.

**Palavras-chave:** *Zea mays*, sonificação, difusividade efetiva, energia de ativação



## INTRODUCTION

Brazil is among the top five corn producers in the world, jointly responsible for approximately 75% of the 2023/2024 harvest production (1,225.452 million tons). The largest producer of this cereal is the United States, responsible for 32% of world production, followed by China (23%), Brazil (11%), the European Union (5%), and Argentina (3%). Of the Brazilian production, the Central-West region contributed with a quantity of 53% (CONAB, 2024).

Corn has an important role in food production, given the wide range of corn-based food products, such as different baked goods, snacks, cakes and cookies, breakfast cereals, porridges, beverages, among others. Field corn has a chemical composition, on a dry basis, of 61 to 78% starch, non-starch polysaccharides (around 10%), proteins (6 to 12%), and lipids (3 to 6%). In this cereal, the intracellular space in the endosperm is occupied by starch granules, which are surrounded by a protein matrix (Zhang et al., 2021).

Corn starch is widely used in the food industry due to its multifunctional properties, such as thickening capacity, stability, gelling, and texturizing in products like sauces, soups, breads, dairy formulations, and gluten-free items. Moreover, its versatility and neutral flavor make it essential for improving the consistency and shelf life of processed foods (Vela et al., 2024).

Starches are formed by two types of glucose polymers, amylose and amylopectin. Amylose consists of a linear chain with few branches. However, amylopectin has numerous branches. This branched structure of amylopectin gives starch properties such as viscosity, gel-forming capacity, and water retention capacity. However, it also has low resistance to high temperature, shear, and digestion, low emulsifying power, low solubility in cold water, a high degree of retrogradation, and instability in acids. Thus, starches are modified to overcome these disadvantages and increase their use in various industrial applications (Yang et al., 2019; Tao et al., 2020; Han et al., 2021; Oyeyinka et al., 2021; Xu et al., 2021).

Ultrasonic technology is useful in modifying the functional physicochemical properties of starch, as it has many advantages such as greater selectivity and quality, lower use of chemicals, and short processing time (Wang et al., 2023a; Taques et al., 2024). The mechanism underlying these changes is mainly attributed to acoustic cavitation, in which the collapse of microbubbles generates localized high pressure and temperature gradients that disrupt the granular structure, promote depolymerization, and alter the crystalline–amorphous balance of starch (Zheng et al., 2020). The extent of these modifications is highly dependent on ultrasonic parameters such as frequency, power, and amplitude, which need to be carefully optimized for each application.

Conversely, the drying stage plays a crucial role in preserving starch quality, as it directly affects its physicochemical and technological properties. In the case of ultrasonically modified starch, drying assumes particular relevance, since structural changes induced by cavitation can influence water retention, gelatinization behavior, and retrogradation, potentially altering the efficiency of conventional drying methods. A proper understanding of drying kinetics, supported by mathematical

modeling, is essential to optimize processing conditions, minimize energy consumption, and ensure high-quality products (Rahaman et al., 2021).

Despite the increasing number of studies on ultrasound-assisted starch modification, little attention has been given to how subsequent drying processes affect the structure and technological properties of ultrasonically treated starch. This gap highlights the need to investigate the combined effects of ultrasound treatment and drying, providing insights into process optimization and product quality. Thus, the objective was to evaluate how ultrasonic modification affects the drying kinetics and technological properties of corn starch, determining optimal drying conditions to preserve functional characteristics.

## MATERIAL AND METHODS

Yellow dent corn grains cultivated in Campo Verde-MT (15° 32' 48" S, 55° 10' 08" W; 736 m a.s.l.), in 2022, were used for the extraction of starch. The starch was extracted and modified using ultrasonic energy according to Taques et al. (2024). Corn kernels were steeped in a 0.2% sodium metabisulfite solution (1:3, w/v) for 48 hours, resuspended in distilled water, and ground in a domestic blender. The slurry was sonicated in an ultrasonic bath (Eco-sonics, Q5.9/40) at 40 kHz frequency, 60% amplitude for 60 min at 25 °C followed by successive washing and sieving with distilled water (No. 100 and No. 270 sieves). Retained fractions were resuspended, re-sonicated under the same conditions, and centrifuged at 4500 rpm for 20 min. The supernatant was discarded and the protein layer on the starch was removed.

The drying of corn starch was conducted in a forced circulation oven (Nova Ética, model 400-3ND), using corn starch with an initial moisture content of  $0.87 \pm 0.02$  (decimal, dry basis), until reaching a final moisture content of  $0.14 \pm 0.005$  (decimal, dry basis), at temperatures of 40, 50, 60, and 70 °C and relative humidities of 27.97, 17.58, 10.85, and 7.19%, respectively. The drying was conducted in a completely randomized design, with four treatments and three replications, so all drying curves were obtained in triplicate. The initial moisture content was determined by the oven method at a temperature of  $105 \pm 2$  °C for 24 hours.

Drying was performed in four cylindrical, non-perforated, metallic trays (120 mm diameter × 49 mm height), each loaded with 50 g of product spread in thin layers (10 mm). With the use of non-perforated trays, the flow of hot, dry air is directed towards the top of the material, promoting gradual evaporation of moisture. The restriction of drying on the bottom layer of the starch allows the internal moisture to slowly migrate to the surface. This results in a more uniform drying rate, which prevents case hardening. Moisture loss was monitored by weighing the samples at 10-min intervals under each drying condition, using a semi-analytical scale (Shimadzu, model BL3200H) with a resolution of 0.01 g, until a constant mass was reached, corresponding to the equilibrium moisture content. After defining the equilibrium moisture contents, the second stage was carried out, where the starch was again subjected to drying until reaching the final moisture content of 0.14 (decimal, dry basis) in order to

evaluate the effect of drying on the technological quality. To evaluate the effect of drying the ultrasound-modified starch, the drying rate was determined using Eq. 1.

$$DR = \frac{X_0 - X_i}{t_i - t_0} \quad (1)$$

Where:

DR - drying rate ( $\text{kg kg}^{-1} \text{h}^{-1}$ );

$X_0$  - previous moisture content (decimal, dry basis);

$X_i$  - current moisture content (decimal, dry basis);

$t_0$  - previous total drying time (hours); and,

$t_i$  - current total drying time (hours).

The experimental data of the drying kinetics were used to calculate the moisture ratio (RX) using Eq. 2.

$$RX = \frac{X - X_e}{X_i - X_e} \quad (2)$$

Where:

X - moisture content of the product, decimal dry basis;

$X_i$  - initial moisture content of the product, decimal dry basis; and,

$X_e$  - equilibrium moisture content of the product, decimal dry basis.

With the experimental data of the moisture ratio, mathematical models frequently employed to represent the drying kinetics of agricultural products (Eqs. 3 to 13, Table 1) were fitted to describe the drying of corn starch extracted and modified via ultrasonic energy.

The experimental data from the drying of corn starch were subjected to non-linear regression analysis by the Gauss-Newton method using Microsoft Excel (Microsoft Corporation, Version 365). The degree of fit of each model was analyzed considering the magnitude of the adjusted coefficient of determination ( $R^2$ ), the relative mean error (P; Eq. 14), and the standard error of estimate (SE; Eq. 15).

$$P = \frac{100}{n} \sum_{i=1}^n \left( \frac{|Y - \hat{Y}|}{Y} \right) \quad (14)$$

$$SE = \sqrt{\frac{\sum_{i=1}^n (Y - \hat{Y})^2}{DF}} \quad (15)$$

Where:

Y - experimental value;

$\hat{Y}$  - value estimated by the model;

n - number of experimental observations; and,

DF - model's degrees of freedom (difference between the number of observations and the number of model parameters).

The Akaike Information Criterion (AIC) and the Schwarz's Bayesian Information Criterion (BIC) (Eqs. 16 and 17) were used to complement the selection of the best-fitting models, subjecting the models pre-adjusted by the Gauss-Newton criterion, commonly used with good acceptance for the selection of best-fitting models for the drying kinetics of various agricultural products (Gomes et al., 2018).

$$AIC = -2\log L + 2p \quad (16)$$

$$BIC = -2\log L + p \ln(n) \quad (17)$$

Where:

p and n - number of parameters and observations of the model; and,

L - maximum likelihood, considering the parameter estimates.

The effective diffusion coefficient was determined based on the fitting of the liquid diffusion mathematical model (Eq. 18) to the experimental starch drying data, considering the geometric shape of an infinite flat plate with an eight-term approximation and the boundary condition of known

**Table 1.** Mathematical models used to describe the drying kinetics of corn starch under different air conditions

Model	Model designation	
Wang & Singh	$RX = 1 + at + bt^2$	(3)
Verma	$RX = -a \exp(-kt) + (1 - a)\exp(-k_1t)$	(4)
Thompson	$RX = \exp\{-a - (a^2 + 4bt)^{0.5}/2b\}$	(5)
Page	$RX = \exp(-kt^n)$	(6)
Newton	$RX = \exp(-kt)$	(7)
Midilli	$RX = a \exp(-kt^n) + bt$	(8)
Logarithmic	$RX = a \exp(-kt) + c$	(9)
Henderson & Pabis	$RX = a \exp(-kt)$	(10)
Two-term exponential	$RX = a \exp(-kt) + (1 - a) \exp(-kat)$	(11)
Two terms	$RX = a \exp(-k_0t) + b \exp(-k_1t)$	(12)
Approximation of diffusion	$RX = a \exp(-kt) + (1 - a) \exp(-kbt)$	(13)

t - Drying time, h; k,  $k_0$ ,  $k_1$  - Drying parameters,  $\text{h}^{-1}$ ; a, b, c, d, n - Model coefficients

moisture content on the product surface (Brooker et al., 1992).

$$RX = \frac{X - X_e}{X_i - X_e} = \frac{6}{\pi^2} \sum_{n_t} \frac{1}{n_t^2} \exp \left[ \frac{n_t^2 \pi^2 D_{\text{eff}} t}{9} \left( \frac{3}{L} \right)^2 \right] \quad (18)$$

Where:

Def - effective diffusion coefficient ( $\text{m}^2 \text{s}^{-1}$ );

t - drying time (hours);

L - thickness of the product (m); and,

n - number of terms in the model.

The trend of the effective diffusion coefficient as a function of the different temperatures applied during the drying process was evaluated using the Arrhenius Equation, described in Eq. 19.

$$D_{\text{ef}} = D_0 \left( \frac{E_a}{RT_a} \right) \quad (19)$$

Where:

Do - pre-exponential factor;

Ea - activation energy,  $\text{kJ mol}^{-1}$ ;

R - universal gas constant,  $8.314 \text{ kJ kmol}^{-1} \text{ K}^{-1}$  (Note: the provided value of 8.134 is slightly different, but 8.314 is the standard value); and,

Ta - absolute temperature, k.

Scanning Electron Microscopy (SEM) was performed at the Multiuser Laboratory of High-Resolution Microscopy of the Federal University of Goiás, using a scanning electron microscope (JSM- 6610/ Jeol<sup>®</sup>), equipped with EDS, ThermoScientific NSS Spectral 1 Imaging. The samples were previously defatted by Soxhlet extraction for 8 hours, as described in AOAC No. 920.39 (AOAC, 2019). This procedure aimed to remove residual lipids and amylose-lipid complexes that could otherwise mask surface features of the granules. The removal of these compounds helps to avoid the formation of thin lipid films, reduces beam-induced artifacts during observation, and ensures clearer visualization of the native morphology. In addition, defatting is a routine procedure reported in starch characterization studies to ensure reproducibility and comparability among samples from different botanical sources (Zhang et al., 2021). The samples were placed on aluminum stubs with double-sided tape, coated with an ultrathin film of gold (electrically conductive material), allowing the operating principle of the SEM by emission of electron beams with an accelerating voltage of 1 kV by a tungsten filament, in order to minimize charging effects commonly observed in non-conductive materials such as starch. In addition, to obtain clearer visualization of the surface morphology and structural features of the starch granules, images were also recorded at 15 kV with a magnification of 5,000 x. The use of both accelerating voltages provided complementary information, allowing a balance between surface resolution and structural contrast.

The thermal properties of the corn starch samples were studied by Differential Scanning Calorimetry (DSC), Netzsch-DSC 204 F1 Nevio model. Samples containing 5 mg of dry basis corn starch and treated with ultrasound were

weighed directly into aluminum pans with sealed lids, and the samples were mixed with the addition of distilled water to obtain an aqueous suspension up to a proportion of 75% water (w/w). The pan was hermetically sealed and allowed to equilibrate for approximately 1 hour before the analysis proceeded. Subsequently, the sample-containing pans were heated from 20 to 100 °C at a rate of 10 °C  $\text{min}^{-1}$ . The onset gelatinization temperature (To), peak temperature (Tp), and conclusion temperature (Tc) were measured.

## RESULTS AND DISCUSSION

The drying process of corn starch was carried out until a final moisture content of  $0.14 \pm 0.005$  (decimal, dry basis) was reached. The times required to reduce the moisture content from  $0.87 \pm 0.02$  (decimal, dry basis) to  $0.14 \pm 0.005$  (decimal, dry basis) were 5.17, 3.17, 2.13, and 1.5 hours for temperatures of 40, 50, 60, and 70 °C, respectively. In general, it is observed that the drying rate decreased with the reduction of air temperature, especially in the initial phase of the process, with reductions over time (Figure 1).

According to Siqueira et al. (2020), the drying time is related to the drying rate, and the higher the drying air temperature, the greater the drying rate and the shorter the time to complete the process. The trend of reducing the drying rate with temperature and drying time has been observed in the drying of various agricultural products, as a result of a greater ease of water removal under high-temperature conditions and higher initial moisture contents, with gradual reductions over time, reflecting the strength with which water is bound to the product.

For corn starch, Ren et al. (2020) showed that higher drying temperatures reduce yield and impair functional properties such as transparency, swelling power, and solubility, while also altering gelatinization and viscosity parameters. Similarly, Wang et al. (2023b) reported structural and thermal changes in starch granules under high-temperature drying. Thus, although higher temperatures improve energy efficiency by shortening drying time and lowering energy use per unit of water removed, they may compromise quality attributes. Lower temperatures, in turn, help preserve starch properties but require longer drying times and greater energy demand, highlighting the need to balance efficiency and quality in corn starch drying.

Table 2 presents the values of the standard error of estimate (SE), mean relative error (P), and coefficient of determination ( $R^2$ ) for the fit of the 11 mathematical models to the thin-layer drying data of starch under the four drying air temperature conditions.

The mean relative error (P) is a statistical parameter that indicates the deviation of the observed values in relation to the curve estimated by the model. According to Mohapatra & Rao (2005), for fitting purposes, P is considered to be an exclusion criterion, with models having P values below 10% being considered adequate. Based on this criterion, for temperatures of 40 and 50 °C, only the Wang & Singh, Verma, Page, Midilli, Logarithmic, and Diffusion Approximation models were suitable. For a temperature of 60 °C, only the Thompson, Newton, and Two-term Exponential models

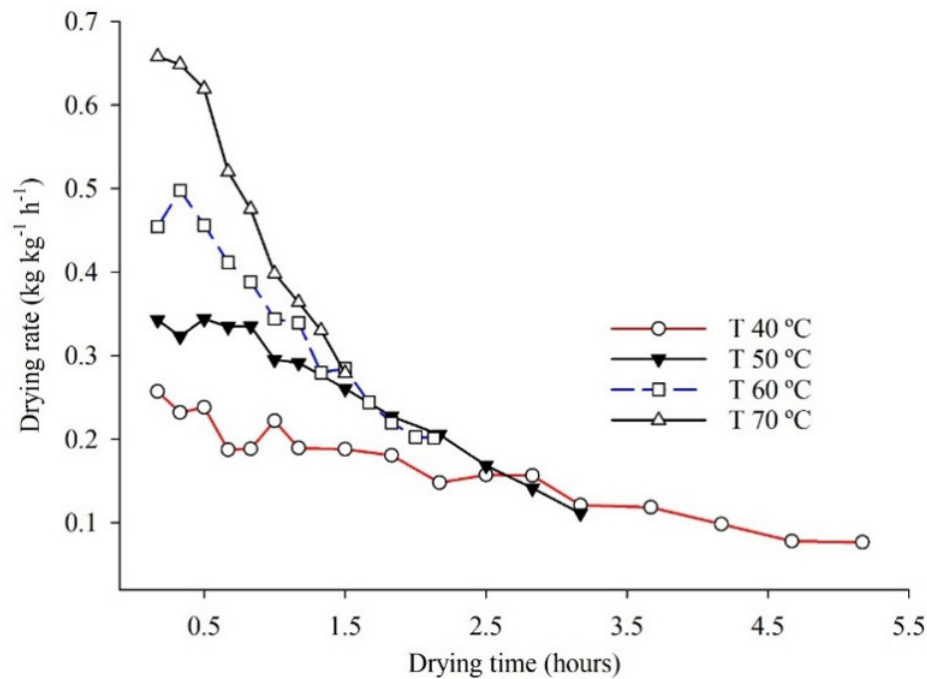


**Figure 1.** Drying rate of corn starch under different temperatures

**Table 2.** Coefficient of determination ( $R^2$ ), mean relative error (P, %), and standard error of estimate (SE, decimal) for the eleven models evaluated in the drying of corn starch at different temperatures ( $^{\circ}\text{C}$ )

Models	Temperatures ( $^{\circ}\text{C}$ )											
	40			50			60			70		
	SE	P (%)	$R^2$	SE	P (%)	$R^2$	SE	P (%)	$R^2$	SE	P(%)	$R^2$
Wang & Singh	0.004	1.132	0.999	0.005	0.853	0.999	0.003	0.734	0.999	0.004	0.695	0.999
Verma	0.018	7.705	0.997	0.009	2.334	0.999	0.011	3.295	0.999	0.009	2.525	0.999
Thompson	0.041	18.192	0.983	0.044	15.440	0.981	0.036	10.959	0.985	0.035	8.948	0.987
Page	0.019	7.884	0.996	0.012	4.092	0.999	0.012	3.445	0.998	0.010	2.707	0.999
Newton	0.040	18.190	0.983	0.042	15.438	0.981	0.035	10.959	0.985	0.033	8.946	0.987
Midilli	0.005	1.362	0.999	0.002	0.664	0.999	0.002	0.324	0.999	0.002	0.326	0.999
Logarithmic	0.005	1.845	0.999	0.008	2.040	0.999	0.004	0.645	0.999	0.005	0.683	0.999
Henderson & Pabis	0.036	15.702	0.987	0.036	12.500	0.987	0.031	9.082	0.990	0.030	7.631	0.991
Two Terms	0.038	15.703	0.987	0.012	3.972	0.999	0.034	9.082	0.990	0.005	0.572	0.999
Two-term Exponential	0.041	18.190	0.983	0.044	15.438	0.981	0.036	10.959	0.985	0.035	8.946	0.987
Diffusion Approximation	0.005	1.568	0.999	0.012	4.138	0.999	0.011	3.295	0.999	0.009	2.525	0.999

were excluded. And at a temperature of  $70^{\circ}\text{C}$ , all models are recommended to represent the drying of corn starch. Complementarily, the values of SE and  $R^2$  are also used, with models that have lower SE values and  $R^2$  greater than 0.95 being considered as having a good fit. From this perspective, it can be observed that in all situations where P was favorable, the  $R^2$  values are greater than 0.95, with most ranging from 0.98 to 0.99. Regarding the SE values, for the temperature of  $40^{\circ}\text{C}$ , the Wang & Singh model stands out, and the Midilli model stands out for the temperatures of 50, 60, and  $70^{\circ}\text{C}$ .

To improve the accuracy in the selection of models, given that SE and  $R^2$  are not mutually exclusive, the Akaike Information Criterion (AIC) and the Schwarz's Bayesian Information Criterion (BIC) were used, reducing potential inaccuracies generated by the previous criteria. Table 3 presents the AIC and BIC values for the models pre-selected by the P, SE, and  $R^2$  criteria for each corn starch drying temperature condition.

The AIC and BIC criteria have been adopted as supplementary because they allow for the selection of only

a single model, with the model that has the highest absolute values for the AIC and BIC criteria being considered well-fitted. In this context, the Wang & Singh model had the highest absolute values at a temperature of 40 °C, and the Midilli model had the highest absolute values at temperatures of 50, 60, and 70 °C (Table 3).

Figure 2 shows the drying curves of corn starch, represented by the Wang & Singh model for the temperature of 40 °C and the Midilli model for the temperatures of 50, 60, and 70 °C.

The selected models show a good fit to describe the starch drying process. A good approximation can be observed between the experimental and estimated values, where the trend line of the model completely overlaps the experimental data. Table 4 presents the parameter values of the Wang & Singh model at 40 °C and the Midilli model at 50, 60, and 70 °C, fitted to the starch drying process.

For the Midilli model, it can be observed that the magnitude of the drying constant ( $k$ ) increases with the elevation of the drying air temperature, while the other parameters showed a random trend. The parameter " $k$ " can be used as an approximation to characterize the effect of temperature and is related to the effective diffusivity in the falling rate period of the drying process, with liquid diffusion controlling the drying process (Moura et al., 2021). This behavior has been observed in other studies on the mathematical modeling of the drying of various agricultural products, such as those by Siqueira et al. (2020) and Ferreira Junior et al. (2021).

The activation energy and the effective diffusion coefficient are important parameters that help in understanding the drying of agricultural raw materials. By

relating these concepts to temperature, the nature of the material, and other factors, it is possible to optimize these processes. Figure 3 shows the values of the effective diffusion coefficient and activation energy, as well as the Arrhenius representation for the starch drying process. The equation was fitted to the experimental drying data based on Fick's Second Law, considering the geometric shape of an infinite flat plate with an average layer thickness of  $8.76 \pm 0.76$  mm.

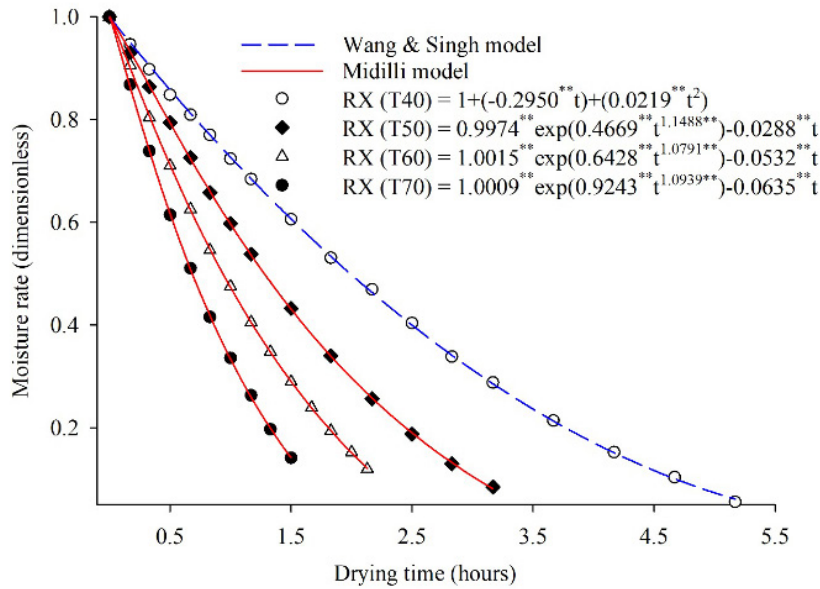
Diffusivity can be understood as the ease with which water is removed from the agricultural product (Gomes et al., 2018). Thus, a higher effective diffusion coefficient indicates a higher drying rate, as water molecules move more quickly to the surface to evaporate due to the energy exchange with the hot drying air. Furthermore, the higher the effective diffusion coefficient, the lower the activation energy, since the activation energy represents the minimum amount of energy required for a water molecule within a moist material to overcome intermolecular forces and diffuse to the surface (Gomes et al., 2018; Cavalcanti-Mata et al., 2020). The effective diffusion coefficient increased linearly with the increase in drying air temperature, ranging from  $2.4066 \times 10^{-9}$  to  $7.1088 \times 10^{-9}$   $\text{m}^2 \text{s}^{-1}$  for the temperature range of 40 to 70 °C, respectively (Figure 3B). The reduction in temperature increases the internal resistance to water diffusion necessary to trigger the water evaporation process in the product. Consequently, higher values of the effective diffusion coefficient were observed for higher drying air temperatures.

The activation energy for the drying of corn starch at temperatures of 40, 50, 60, and 70 °C was  $32.25 \text{ kJ mol}^{-1}$ , and is consistent with values reported in the literature for corn and starch-based products. Ononogbo et al. (2021) reported activation energies ranging from 31.75 to  $41.05 \text{ kJ mol}^{-1}$  for

**Table 3.** Akaike information criterion (AIC) and Schwarz's Bayesian information criterion (BIC) for the models that best fit the starch drying data under different drying air temperature conditions

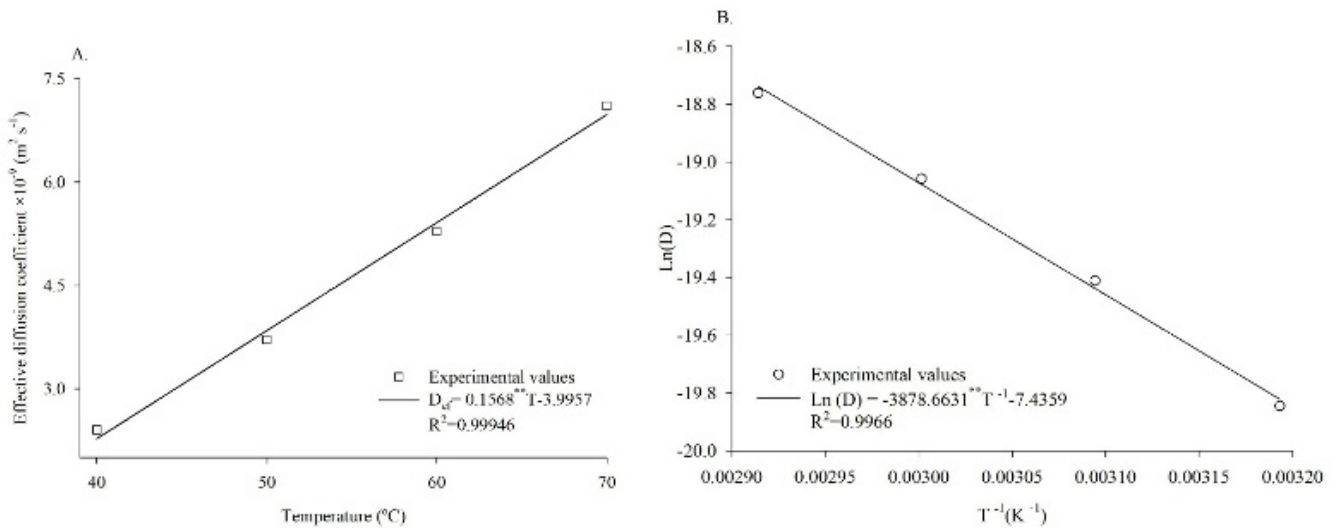
Models	Temperatures (°C)							
	40		50		60		70	
	AIC	BIC	AIC	BIC	AIC	BIC	AIC	BIC
Wang & Singh	-142.79	-140.12	-106.64	-104.72	-116.93	-115.02	-80.61	-79.70
Verma	NA	NA	NA	NA	NA	NA	NA	NA
Thompson	-	-	-	-	-	-	NA	NA
Page	-87.38	-84.71	-79.84	-77.92	-80.77	-78.85	-59.88	-58.97
Newton	-	-	-	-	-51.24	-49.96	-37.01	-36.41
Midilli	-135.65	-131.20	-123.01	-119.81	-134.65	-131.46	-92.59	-91.08
Logarithmic	-133.72	-130.16	-91.46	-88.91	-111.21	-108.66	-73.35	-72.14
Henderson & Pabis	-	-	-	-	-54.07	-52.15	-38.03	-37.12
Two Terms	-	-	NA	NA	NA	NA	NA	NA
Two-term Exponential	-	-	-	-	-	-	NA	NA
Diffusion Approximation	NA	NA	NA	NA	NA	NA	NA	NA

NA - Values not applicable by the AIC and BIC criteria; - Models excluded by the previous criteria



\*\*Significant at  $p < 0.01$

**Figure 2.** Moisture ratio values obtained experimentally and estimated by the Wang & Singh model at 40 °C and the Midilli model at 50, 60, and 70 °C for the drying of corn starch modified by ultrasonic energy



\*\*Significant at  $p < 0.01$

**Figure 3.** Average values of the effective diffusion coefficient (A) and the Arrhenius representation (B) for the drying of starch at temperatures of 40, 50, 60, and 70 °C

**Table 4.** Coefficients of the Wang & Singh and Midilli models obtained for starch subjected to drying under different drying air conditions

Temperatures (°C)	Mathematical models					
	Midilli				Wang & Singh	
	a	k	b	n	a	b
40	-	-	-	-	-0.294*	0.022*
50	0.997*	0.467*	-0.029*	1.149*	-	-
60	1.001*	0.644*	-0.053*	1.081*	-	-
70	1.001*	0.922*	-0.064*	1.093*	-	-

\*Significant effect ( $p < 0.05$ , Student's t-test)

thin-layer drying of maize. These comparisons confirm that the activation energy calculated in the present work falls within the expected range, supporting the reliability of the kinetic modeling applied.

Figure 4 shows the scanning electron microscopy images of corn starch obtained by the ultrasonic method and dehydrated at temperatures of 40, 50, 60, and 70 °C. It can be observed that, for all drying temperatures, the starch granules exhibit polyhedral and rounded shapes, which are characteristic of corn starch. The size and shape of starch granules are related to their source (Wang et al., 2021).

The size of starch granules (200 - 300 granules) when subjected to drying at a temperature of 40 °C was 0.0149 mm, at 50 °C it was 0.0146 mm, at 60 °C it was 0.0143 mm, and at 70 °C it was 0.0135 mm. It is observed that the starch granules are broken and the starch is fragmented. Larger granules are also observed in the starch subjected to a drying temperature of 40 °C, compared to the other temperatures, which led to a greater quantity of smaller and fragmented granules. According to Liu et al. (2009), with the increase in temperature, the hydrogen bonds are broken and the

molecules combine with the hydroxyl group of the starch molecules. This process leads to the dissolution of starch crystals and the fragmentation of the granules. In this phase, the double helix structure of amylopectin is dissociated and destroyed, followed by the fragmentation of the starch, making them smaller. The results of differential scanning calorimetry of corn starch subjected to different drying temperatures are presented in Table 5.

For samples dried at 40 and 50 °C, endothermic gelatinization events were observed with  $T_o \approx 45.6\text{--}46.1$  °C,  $T_p \approx 51.8$  °C, and  $T_c \approx 55.9\text{--}56.8$  °C, indicating partial preservation of crystalline order. In contrast, samples dried at 60 and 70 °C showed no detectable gelatinization peaks within the scanned range (Table 5).

For starches dried at 60 and 70 °C, no peaks were observed in the DSC thermograms, indicating the absence of a thermal event. The absence of endothermic gelatinization peaks in corn starch subjected to high-temperature drying can be explained by prior structural modifications that eliminated or sufficiently reduced the crystalline order required to generate transitions detectable by DSC. According to Zhao et al. (2024),

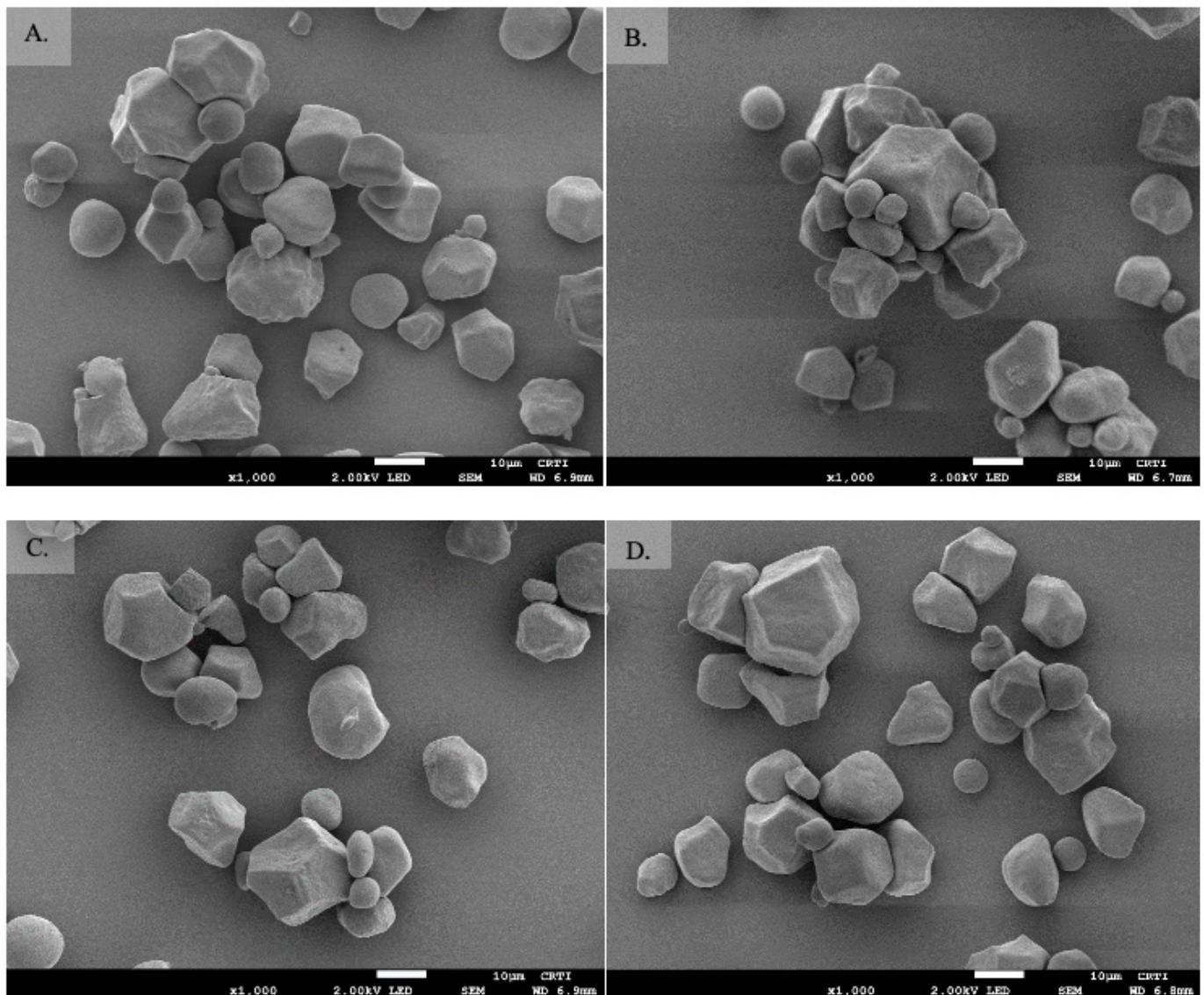


**Figure 4.** Scanning Electron Microscopy of corn starch obtained by ultrasonic extraction and dehydrated at temperatures of 40 (A), 50 (B), 60 (C), and 70 °C (D)

**Table 5.** Onset (To), peak (Tp), and conclusion (Tc) gelatinization temperatures of corn starch suspensions after drying at 40, 50, 60, and 70 °C

Temperatures (°C)	To	Tp	Tc
40	45.6	51.8	56.8
50	46.1	51.8	55.9
60	-	-	-
70	-	-	-

- no detectable gelatinization peak within the analyzed range. To - Onset; Tp - Peak; Tc - Conclusion

this may be due to the loss of double-helical linkages through pre-gelatinization during the starch drying process. Pre-gelatinized starches consist of damaged granules, are soluble in water at room temperature, and exhibit crystalline disorder, since depolymerization or fragmentation of starch molecules can occur during this process (Moraes et al., 2013; Roa et al., 2014). Studies have shown that thermal treatments or severe drying processes can induce crystalline reorganization, loss of crystallinity, or collapse of the crystalline regions of starch granules (Mao et al., 2023). In addition, under low-hydration conditions, starch may not display gelatinization peaks (Bertrand et al., 2019), because without sufficient water to plasticize the matrix and disrupt hydrogen bonds, starch may show no peak even at elevated temperatures (Chiodetti et al., 2024). Furthermore, severe thermal treatments such as drying can lead to prior gelatinization or degradation of crystalline order, so that during the calorimetric scan there is no remaining transition enthalpy to be recorded (the endotherm disappears). The study by Téllez-Morales et al. (2025) shows that extrusion of mixtures containing corn starch yielded 100% gelatinization and the absence of an endotherm in the DSC.

Regarding technological and industrial properties, the absence of a gelatinization endotherm at higher drying temperatures indicates reduced gelatinization capacity, with decreases in swelling power, solubility, and paste viscosity, directly impacting applications such as sauces, creams, fillings, and bakery products. Conversely, such pre-modified starches may contribute to greater thermal stability, as they can resist unwanted gelatinization under severe thermal processing, thereby reducing syneresis/retrogradation, which is advantageous for sterilized or long-shelf-life products (Marta et al., 2022).

The gelatinization temperature obtained was lower than that described in the literature. Drying can disrupt crystalline lamellae and amylopectin double-helical structures (Dome et al., 2020; Cheng et al., 2024), increasing the fraction of disordered amorphous regions. These regions are more easily hydrated, thereby enabling gelatinization at lower temperatures (Song et al., 2017; Ye & Baik, 2024). Weber et al. (2009) observed that the gelatinization temperature of corn starch with 27.8% amylose was 77.26 °C. Rahaman et al. (2021) also observed gelatinization at 77.72 °C for corn starch subjected to ultrasonic treatment for 20 min. However, this reduction in gelatinization temperature may be due to the physical modification promoted by the use of ultrasound treatment.

Gelatinization at higher temperatures is due to a higher degree of crystallinity of the starch, which provides thermal stability against gelatinization (Abdullah et al., 2018). In addition, the presence of cracks and pores on the surface of the modified starch can facilitate water penetration into the granules, breaking the crystalline regions and consequently reducing the gelatinization temperature of the starch (Sujka, 2017; Yang et al., 2019; Fashi et al., 2023). The presence of cracks and pores was observed in the modified starch as reported by Taques et al. (2024). Another factor that may have contributed to a lower gelatinization temperature is the fact that crystallinity is influenced by the chain length of amylopectin, with smaller granules resulting in higher gelatinization temperatures (Abdullah et al., 2018). The SEM results showed that drying at lower temperatures resulted in starches with larger granules and, consequently, lower gelatinization temperatures. Other researchers have also obtained a reduction in the gelatinization temperature of corn starch when it was subjected to ultrasonic treatment. Fashi et al. (2023) observed a slight reduction in the peak gelatinization temperature from 71.11 to 69.94 °C for native and sonicated starch, respectively.

## CONCLUSIONS

Drying of ultrasound-modified corn starch was successfully described by the Wang & Singh model at 40 °C and the Midilli model at 50–70 °C. The effective moisture diffusivity increased linearly with temperature ( $2.41 \times 10^{-9}$  to  $7.11 \times 10^{-9}$  m<sup>2</sup> s<sup>-1</sup>), yielding an activation energy of 32.25 kJ mol<sup>-1</sup>.

1. Morphologically, granule size decreased with temperature and evidence of fragmentation was observed.
2. Drying preserved the gelatinization behavior of starch dried at 40 and 50 °C. For starches dried at 60 and 70 °C, no peaks were observed in the DSC thermogram, indicating the absence of a thermal event.
3. From a practical perspective, these findings suggest that drying at controlled temperatures, preferably below 50 °C, allows the production of starch with more stable functional properties, broadening its industrial applications.

**Contribution of authors:** Aparecida S. Taques: Conceptualization, Formal analysis, Methodology, Writing original draft, Writing - review & editing. Juliana A. Célia: Formal analysis, Investigation, Methodology. Daniel E. C. de Oliveira: Drying analysis, Investigation, Methodology. Geraldo A. Mabasso: Formal analysis, Investigation. Raquel A. Loss: Supervision, Validation, Writing - review & editing. Osvaldo Resende: Supervision, Validation, Writing - review & editing.

**Data Availability Statement:** The authors declare that there are no data underlying the text.

**Conflict of Interest:** There are no conflict of interest.

**Financing statement:** Instituto Federal do Mato Grosso Dinter Process: 23216.001441.2022-12.

**Acknowledgements:** The authors extend thanks to Instituto Federal Goiano (Dinter Process: 23216.001441.2022-12), Instituto Federal do Mato Grosso and Universidade do Estado de Mato Grosso (UNEMAT) - Campus Barra do Bugres, through structural support. To CAPES, FAPEG,

FINEP, Embrapii and CNPq (Process: 310222/2021-4), for their financial support, which was indispensable to the execution of this study.

### LITERATURE CITED

- Abdullah, A. H. D.; Chalimah, S.; Primadona, I.; Hanantyo, M. H. G. Physical and chemical properties of corn, cassava, and potato starches. IOP Conf. Series: Earth and Environmental Science, v.160, 012003, 2018. <https://doi.org/10.1088/1755-1315/160/1/012003>
- AOAC - Official Methods of Analysis, 21<sup>st</sup> Edition. Available on: <https://www.aoac.org/official-methods-of-analysis-21st-edition-2019/>. Accessed in: Aug. 2024.
- Bertrand, R.; Holmes, W.; Orgeron, C.; McIntyre, C.; Hernandez, R.; Revellame, E. D. Rapid estimation of parameters for gelatinization of waxy corn starch. Foods, v.6, e556, 2019. <https://doi.org/10.3390/foods8110556>
- Brooker, D. B.; Bakker-Arkema F. W.; Hall, C. W. Drying and storage of grains and oilseeds Westport. Nova York: The AVI Publishing Company, 1992, 76p.
- Cavalcanti-Mata, M. E. R. M.; Duarte, M. E. M.; Lira, V. V.; Oliveira, R. F. de; Costa, N. L.; Oliveira, H. M. L. A new approach to the traditional drying models for the thin-layer drying kinetics of chickpeas. Journal of Food Process Engineering, v.43, e1356, 2020. <https://doi.org/10.1111/jfpe.13569>
- Cheng, J. Insight into characteristics in rice starch under heat-moisture treatment: Focus on the structure of amylose/amylopectin. Food Chemistry, v.24, e10194, 2024. <https://doi.org/10.1016/j.fochx.2024.101942>
- Chiodett, M.; Tuccio, M. G.; Carini, L. Effect of water content on gelatinization functionality of flour from sprouted sorghum. Current Research in Food Science, v.8, e100780, 2024. <https://doi.org/10.1016/j.crfs.2024.100780>
- CONAB - Companhia Nacional de Abastecimento. Acompanhamento da safra brasileira de grãos: safra 2023/2024. Available on: <https://www.conab.gov.br/info-agro/safra/safraos>. Accessed in: Jul. 2024.
- Dome, K.; Podgorbunskikh, E.; Bychkov, A.; Lomovsky, O. Changes in the Crystallinity degree of starch having different types of crystal structure after mechanical pretreatment. Polymers, v.12, e641, 2020. <https://doi.org/10.3390/polym12030641>
- Fashi, A.; Delavar, A. F.; Zamani, A.; Noshiranzadeh, N.; Zahraei, H. Study on structural and physicochemical properties of modified corn starch: Comparison of ultrasound, stirring, and lactic acid treatments. Starch – Stärke, v.75, p.1-9, 2023. <https://doi.org/10.1002/star.202200109>
- Ferreira Junior, W. N.; Resende, O.; Pinheiro, G. K. I.; Silva, L. C. M.; Souza, D. G.; Sousa, K. A. Modeling and thermodynamic properties of the drying of tamarind (*Tamarindus indica* L.) seeds. Revista Brasileira de Engenharia Agrícola e Ambiental, v.25, p.37-44, 2021. <https://doi.org/10.1590/1807-1929/agriambi.v25n1p37-43>
- Gomes, F. P.; Resende, O.; Sousa, E. P.; Oliveira, D. E. C.; Araújo Neto, F. R. de Drying kinetics of crushed mass of 'jambu': Effective diffusivity and activation energy. Revista Brasileira de Engenharia Agrícola e Ambiental, v.22, p.499-505, 2018. <https://doi.org/10.1590/1807-1929/agriambi.v22n7p499-505>
- Han, Z.; Li, Y.; Luo, D. H.; Zhao, Q.; Cheng, J. H.; Wang, J. H. Structural variations of rice starch affected by constant power microwave treatment. Food Chemistry, v.359, e129887, 2021. <https://doi.org/10.1016/j.foodchem.2021.129887>
- Huang, Z. Q.; Xie, X. L.; Chen, Y.; Lu, J. P.; Zhang-Fa Tong, Z. F. Ball-milling treatment effect on physicochemical properties and features for cassava and maize starches. Journals Rendus Chimies, v.11, p.73-79, 2008. <https://doi.org/10.1016/j.crci.2007.04.008>
- Jodicke, K.; Arendt, S.; Hofacker, W.; Speckle, W. The influence of process parameters on the quality of dried agricultural products determined using the cumulated thermal load. Drying Technology, v.8, p.321-332, 2019. <https://doi.org/10.1080/07373937.2019.1568254>
- Liu, H.; Xie, F.; Yu, L.; Chen, L.; Lia, L. Thermal processing of starch-based polymers, Progress in Polymer Science, v.34, p.1348-1368, 2009. <https://doi.org/10.1016/j.progpolymsci.2009.07.001>
- Mao, L.; Mhaske, P.; Farahnaky, A.; Majzoobi, M. Effect of dry heating on some physicochemical properties of protein-coated high amylose and waxy corn starch. Foods, v.12, e1350, 2023. <https://doi.org/10.3390/foods1206135>
- Marta, H.; Cahyana, Y.; Bintang, S.; Soeherman, G. P.; Djali, M. Propriedades físico-químicas e de pasta do amido de milho afetadas pela modificação hidrotérmica por vários métodos. Revista Internacional de Propriedades Alimentares, v.25, p.792-812, 2022. <https://doi.org/10.1080/10942912.2022.2064490>
- Microsoft Corporation. Microsoft Excel [software]. Version 365. Redmond: Microsoft Corporation, 2023.
- Mohapatra, D.; Rao, P. S. A thin layer-drying model of parboiled wheat. Journal of Food Engineering, v.66, p.513-518, 2005. <https://doi.org/10.1016/j.jfoodeng.2004.04.023>
- Moraes, J.; Alves, F. S.; Franco, C. M. L. Effect of ball milling on structural and physicochemical characteristics of cassava and Peruvian carrot starches. Starch-Stärke, v.65, p.200-209, 2013. <https://doi.org/10.1002/star.201200059>
- Moura, H. V.; Figueirêdo, R. M. F. de; Queiroz, A. F. de M.; Silva, E. T. de V.; Esmero, J. A. D.; Lisboa, J. A. D. Mathematical modeling and thermodynamic properties of the drying kinetics of trapiá residues. Journal of Food Process Engineering, v.44, e13768, 2021. <https://doi.org/10.1111/jfpe.13768>
- Ononogbo, C.; Nwufu, O. C.; Nwakuba, N. R.; Okoronkwo, C. A.; Igbokwe, J. O.; Nwadinobi, P. C.; Anyanwu, E. E. Energy parameters of corn drying in a hot air dryer powered by exhaust gas waste heat: An optimization case study of the food-energy nexus. Energy Nexus, v.4, 100029, 2021. <https://doi.org/10.1016/j.nexus.2021.100029>
- Oyeyinka, S. A.; Akintayo, O. A.; Adebo, O. A.; Kayitesi, E.; Njobeh, P. B. A review on the physicochemical properties of starches modified by microwave alone and in combination with other methods. International Journal of Biological Macromolecules, v.176, p.87-95, 2021. <https://doi.org/10.1016/j.ijbiomac.2021.02.066>
- Rahaman, A.; Kumari, A.; Zeng, X. A.; Farooq, M. A.; Siddique, R.; Khalifa, I.; Siddeeg, A.; Ali, M.; Manzoor, M. F. Ultrasound based modification and structural-functional analysis of corn and cassava starch. Ultrasonic Sonochemistry, v.80, e105795, 2021. <https://doi.org/10.1016/j.ultsonch.2021.105795>
- Ren, G.; Zhang, L.; Zeng, F.; Li, Y.; Li, L.; Duan, X. Effects of hot air drying temperature and tempering time on the properties of maize starch. International Journal of Agricultural and Biological Engineering, v.13, p.236-241, 2020. <https://doi.org/10.25165/j.ijabe.20201306.3362>
- Roa, D. F. Santagapita, P. R.; Buera, M. P.; Tolaba, M. P. Ball milling of amaranth starch-enriched fraction: Changes on particle size, starch crystallinity, and functionality as a function of milling energy. Food and Bioprocess Technology, v.7, p.2723-2731, 2014. <https://doi.org/10.1007/s11947-014-1283-0>

- Siqueira, V. C.; Leite, R. A.; Mabasso, G. A.; Martins, E. A. S.; Quequeto, W. D.; Isquierdo, E. P. Drying kinetics and effective diffusion of buckwheat grains. *Ciência e Agrotecnologia*, v.44, e011320, 2020. <http://dx.doi.org/10.1590/1413-7054202044011320>
- Song, M.; Choi, S. H.; Seon-Min Oh, S. M.; Kim, H. Y.; Bae, J. E.; Parque, C. S.; Kim, Y.; Baik, M. Y. Characterization of amorphous granular starches prepared by high hydrostatic pressure (HHP). *Journal of Food Science and Biotechnology* v.54, p.671-678, 2017. <https://doi.org/10.1007/s10068-017-0106-2>
- Sujka, M. Ultrasonic modification of starch – Impact on granules porosity. *Ultrasonics Sonochemistry*, v.37, p.424-429, 2017. <https://doi.org/10.1016/j.ultsonch.2017.02.001>
- Tao, Y.; Yan, B.; Fan, D.; Zhang, N.; Ma, S.; Wang, L.; Wu, Y.; Wang, M.; Zhao, J.; Zhang, H. Structural changes of starch subjected to microwave heating: A review from the perspective of dielectric properties. *Trends in Food Science & Technology*, v.99, p.593-607, 2020. <https://doi.org/10.1016/j.tifs.2020.02.020>
- Taques, A. S.; Célia, J. A.; Almeida, J. S. de; Ferreira, M. N.; Loss, R. A.; Resende, O. Efeito do ultrassom na extração e modificação do amido de milho (*Zea mays*). *Revista Caderno Pedagógico*, v.21, p.1-21, 2024. <https://doi.org/10.54033/cadpedv21n8-072>
- Télez-Morales, J. A.; Rodríguez-Miranda, J.; Serrano-Villa, F. S.; Calderon-Domínguez, G. Extrusion cooking analysis of corn starch and WPI mixture as a model system on the microstructure and thermodynamic parameters. *LWT – Food Science and Technology*, v.226, 117963, 2025. <https://doi.org/10.1016/j.lwt.2025.117963>
- Vela, A. J.; Villanueva, M.; Ronda, F. R. Ultrasonication: An Efficient Alternative for the Physical Modification of Starches, Flours and Grains. *Foods*, v.13, e2325, 2024. <https://doi.org/10.3390/foods13152325>
- Wang, B.; Gao, W.; Kang, X.; Dong, Y.; Liu, P.; Yan, S.; Yu, B.; Guo, L.; Cui, B.; El-Aty, A. M. Structural changes in corn starch granules treated at different temperatures. *Food Hydrocolloids*, v.118, 106760, 2021. <https://doi.org/10.1016/j.foodhyd.2021.106760>
- Wang, B.; Zhong, Z.; Wang, Y.; Yuan, S.; Jiang, Y.; Li, Z.; Li, Y.; Yan, Z.; Meng, L.; Qiu, L. Recent progress of starch modification assisted by ultrasonic wave. *Food Science and Technology*, v.43, e107522, 2023b. <https://doi.org/10.1590/fst.107522>
- Wang, X.; Wang, Y.; Zhao, H.; Tao, H.; Gao, W.; Wu, Z.; Zhang, K.; Bin Yu, B.; Cui, B. Influence of hot-air drying on the starch structure and physicochemical properties of two corn cultivars cultivated in East China. *Journal of Cereal Science*, v.114, e103796, 2023a. <https://doi.org/10.1016/j.jcs.2023.103796>
- Weber, F. H.; Collares-Queiroz, F. P.; Chang, Y. K. Caracterização físico-química, reológica, morfológica e térmica dos amidos de milho normal, ceroso e com alto teor de amilose. *Ciência e Tecnologia de Alimentos*, v.29, p.748-753, 2009. <https://doi.org/10.1590/S0101-20612009000400008>
- Xu, B.; Ren, A.; Chen, J.; Li, H.; Wei, B.; Wang, J.; Azam, S.M.R.; Bhandari, B.; Zhou, C.; Ma, H. Effect of multi-mode dual-frequency ultrasound irradiation on the degradation of waxy corn starch in a gelatinized state. *Food Hydrocolloids*, v.113, e106440, 2021. <https://doi.org/10.1016/j.foodhyd.2020.106440>
- Yang, Q. Y.; Li, X.; Du, X.; Li, F.; Wang, T.; Gao, Y.; Liuc, J.; Luo, X.; Guo, X.; Tang, Z. Fine structure, crystalline and physicochemical properties of waxy corn starch treated by ultrasound irradiation. *Ultrasonic Sonochemistry*, v.51, p.350-358, 2019. <https://doi.org/10.1016/j.ultsonch.2018.09.001>
- Ye, S. J.; Baik, M. Y. Physicochemical properties of amorphous granular starch (AGS) prepared by non-thermal gelatinization by high hydrostatic pressure and spray drying. *International Journal of Biological Macromolecules*, v.260, e129508, 2024. <https://doi.org/10.1016/j.ijbiomac.2024.129508>
- Zhang, B.; Xiao, Y.; Wu, X.; Luo, F.; Lin, Q. L.; Ding, Y. Changes in structural, digestive, and rheological properties of corn, potato, and pea starches as influenced by different ultrasonic treatments. *International Journal of Biological Macromolecules*, v.185, p.206–218, 2021. <https://doi.org/10.1016/j.ijbiomac.2021.06.127>
- Zhao, Y.; Qiao, S.; Zhu, X.; Guo, J.; Peng, G.; Zhu, X.; Gu, R.; Meng, Z.; Zhuona Wu, Z.; Gan, H.; Guifang, D.; Jin, Y.; Liu, S.; Sun, Y. Effect of different drying methods on the structure and properties of porous starch. *Heliyon*, v.10, e31143, 2024. <https://doi.org/10.1016/j.heliyon.2024.e31143>
- Zheng, Y.; Tiana, J.; Kong, X.; Yang, W.; Yin, X.; Xu, E.; Chen, S.; Liu, D.; Sim, X. Physicochemical and digestibility characterization of maize starch-caffeic acid complexes. *LWT-Food Science & Technology*, v.121, e108857, 2020. <https://doi.org/10.1016/j.lwt.2019.108857>